Regional Studies in Marine Science 39 (2020) 101397

Contents lists available at ScienceDirect

Regional Studies in Marine Science

journal homepage: www.elsevier.com/locate/rsma

Wind-driven development and transport of *Gymnodinium catenatum* blooms along the coast of Fujian, China

Caiyun Zhang [a,*], Po-teen Lim [b], Xueding Li [c], Haifeng Gu [d], Xing Li [c], Donald M. Anderson [e]

[a] State Key Laboratory of Marine Environmental Science, College of Ocean and Earth Sciences, Xiamen University, Xiamen 361102, China
[b] Institute of Ocean and Earth Science, University of Malaya, 16310 Bachok Kelantan, Malaysia
[c] Marine Forecasting Center of Fujian Province, Fuzhou, 350003, China
[d] Third Institute of Oceanography, Ministry of Natural Resources, Xiamen 361005, China
[e] Biology Department, Woods Hole Oceanographic Institution, Woods Hole MA 02543, USA

ARTICLE INFO

Article history:
Received 13 February 2020
Received in revised form 27 June 2020
Accepted 10 August 2020
Available online 12 August 2020

Keywords:
Gymnodinium catenatum
Alongshore transport
Physical aggregation
Wind
Fujian coast

ABSTRACT

Gymnodinium catenatum is a cosmopolitan, bloom-forming dinoflagellate known to produce a suite of potent paralytic shellfish poisoning (PSP) toxins. Here, we revisit two major blooms of *G. catenatum* along the Fujianese Coast, China, in 2017 and 2018. The impact area of the 2017 bloom was larger than that of the 2018 event. Field sampling and remote satellite sensing revealed that alongshore transport driven by the southwest wind, as well as physical accumulation driven by the northeast wind, played important roles in the development and distribution of the two bloom events. The relationship between wind-induced hydrodynamic conditions and the unprecedented HAB events established in this study adds greatly to our understanding of algal bloom dynamics along the Fujianese coast. These results improve our ability to detect, track, and forecast *G. catenatum* blooms, thereby potentially minimizing the negative impacts of future HAB events.

© 2020 Elsevier B.V. All rights reserved.

1. Introduction

Harmful algal bloom (HAB) events impact coastal nations worldwide. In many areas, these events are increasing in frequency, distribution, and intensity (Anderson et al., 2012; Hallegraeff, 1993). Such increases have been linked to many different factors, including ballast water transport (Bolch and de Salas, 2007), improved detection capabilities, and the stimulatory effects of anthropogenic nutrient inputs, coastal development, and climate change (Anderson, 1989). Toxic HABs lead to the biotoxin contamination of seafood products (especially shellfish) and threaten the environment, public health, and socio-economic growth of affected areas (Anderson, 1995). Analyses of the bloom dynamics of HAB species in localized settings, as well as their physical–biological interactions, are therefore extremely important.

The unarmored chain-forming dinoflagellate *Gymnodinium catenatum,* which produces paralytic shellfish toxins, was first described from the Gulf of California (Graham, 1943), but this species is globally distributed in temperate, tropical, and equatorial coastal and shelf waters, including those of North and South America (Band-Schmidt et al., 2004; Graham, 1943), Europe (Bravo et al., 2010; Fermín et al., 1996), Australia (Bolch and de Salas, 2007), New Zealand (Mackenzie and Beauchamp, 2001), Japan, and Southeast Asia (Matsuoka and Fukuyo, 1994). In China, *G. catenatum* is distributed in the Pearl River estuary (Qi et al., 1996; Tang et al., 2003) and the Yellow Sea (Gu et al., 2013). *Gymnodinium catenatum* has a cyst stage in its life cycle, and this cyst is characterized by a unique microreticulate surface (Anderson et al., 1988).

The first reported outbreaks of paralytic shellfish poisoning (PSP) attributed to *G. catenatum* occurred in 1976 in Spain (Estrada et al., 1984). Hallegraeff et al. (2012) reviewed *G. catenatum* bloom dynamics in Tasmanian, Spanish/Portuguese, and Mexican waters, and found that this species tolerated a wide range of temperatures and salinities, consistent with the findings of Band-Schmidt et al. (2004). *G. catenatum* has strong vertical migration behaviors (Doblin et al., 2006), which confer a selective advantage on *G. catenatum* in downwelling areas, and in the more turbulent waters surrounding upwelling areas (Moita et al., 2003; Tilstone et al., 1994). Offshore populations of *G. catenatum* have been transported by estuarine circulation or alongshore currents, and have developed into nearshore blooms (Crespo et al., 2007; Fermín et al., 1996; Sordo et al., 2001).

Rapid economic development and intensive coastal aquaculture have led to the serious eutrophication of Chinese coastal waters (Zhou et al., 2008). The frequencies of HABs along the Chinese coast have increased since the 1970s (Yan et al., 2002).

* Correspondence to: College of Ocean and Earth Sciences, Xiamen University, Xiang'an Campus, Xiang'an District, Xiamen, Fujian 361102, China.
E-mail address: cyzhang@xmu.edu.cn (C. Zhang).

https://doi.org/10.1016/j.rsma.2020.101397
2352-4855/© 2020 Elsevier B.V. All rights reserved.

At present, PSP is the most important type of phycotoxin-related poisoning along the Chinese coast; these toxins affect many important shellfish farming areas (Yan et al., 2002; Yu and Luo, 2016). Most PSP events along the Chinese coast have been caused by toxic dinoflagellate species in the genus *Alexandrium* (Yu and Luo, 2016).

In June 2017 and June 2018, two intense *G. catenatum* blooms occurred along the coast of Fujian Province, China. The 2017 bloom event was the first major *G. catenatum* bloom event recorded in Fujianese coastal waters (Chen, 2018). In this event, 36 people in Zhangzhou and eight in Quanzhou City were hospitalized after consuming contaminated mussels (Chen, 2018). These events caused the closure of marine aquaculture farms and led to increased public concern about shellfish safety (Chen, 2018).

Fujian is an important province for marine aquaculture in China, with a marine aquaculture area of 155.74×10^3 ha, and a total aquaculture production of 445.32×10^4 tons in 2017 (FPBS, 2018). Of the total aquaculture production, shellfish represented 283.54×10^4 tons (FPBS, 2018). Thus, the toxic *G. catenatum* bloom caused considerable economic damage to Fujian in 2017.

Fujian is the Chinese province most frequently affected by HABs (Li, 2012), with most HAB events occurring between April and June (Du et al., 2002). During these months, atmospheric forcing of the Taiwan Strait (TWS) transitions from the winter northeast monsoon to the summer southwest monsoon occur as temperature increases gradually (Hong et al., 2011). In the winter, due to the prevailing northeast wind, Zhe-Min Coastal Water (ZMCW) flows southwestward along the coast of Fujian (Zhang and Hong, 2014). This current is characterized by cold, fresh, nutrient-rich waters (Hong et al., 2011). With the strengthening of the southwest monsoon, the influence of the ZMCW weakens, and warm, saline, oligotrophic strait warm water enters the TWS as the South China Sea Warm Current (SCSWC) and the Kuroshio Branch Water (KBW) (Fig. 1) (Hu et al., 2010; Zhang et al., 2011). Meanwhile, the associated wind patterns induce coastal upwelling along the Fujian coast (Hong et al., 2009), which leads to high concentrations of chlorophyll *a* (Chl *a*) in coastal waters. Furthermore, the Min, Jin, and Jiulong Rivers, located in the western TWS (Fig. 1), carry nutrients into the TWS during the spring flood season. Therefore, in the late spring and early summer, the western TWS (i.e., the Fujian coast) has a mild climate and nutrient-rich water, providing suitable conditions for phytoplankton growth (Du et al., 2002; Li, 2012).

In this study, we aim to characterize the key differences between the 2017 and 2018 blooms and then to identify the environmental factors that led to these differences, especially with respect to the role of wind in the transport and development of *G. catenatum* blooms along the Fujianese coast. To address these aims, we first describe the general characteristics of the *G. catenatum* blooms in June 2017 and June 2018 based on field observations and satellite measurements. Then, we examine the relationships between hydrographic conditions and *G. catenatum* bloom development and transport.

2. Materials and methods

2.1. General characteristics of G. catenatum blooms

When a HAB event occurs along the Fujianese coast, daily HABs disaster information reports are released to the public by the Oceanic and Fishery Bureau of Fujian Province (OFBFJ, http://hyyyj.fujian.gov.cn/xxgk/tzgg/). These reports include the record date, impact area, location, water color, species dominating the HAB event, daily maximum concentration of the dominant HABs species, and the stations where PSP levels exceed the regulatory limit. During the *G. catenatum* blooms reported here (June 7–16, 2017 and June 7–14, 2018), several HAB disaster information reports were released (twelve in 2017 and eight in 2018). The daily variations in *G. catenatum* cell densities and PSP distributions were extracted from these information reports, and are shown in Figs. 2 and 3.

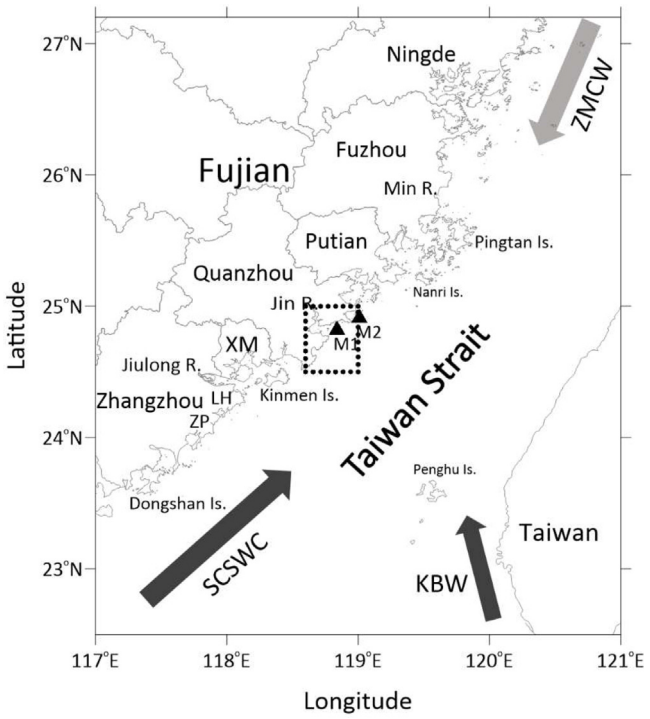

Fig. 1. Schematic map of the study region and the surface water circulation in the Taiwan Strait in late spring and early summer. The solid triangles represent the two mooring stations. The dotted rectangle indicates the geographic extent in Fig.2b. IS: Island; XM: Xiamen; ZP: Zhangpu; LH: Longhai; SCSWC: South China Sea Warm Current; KBW: Kuroshio Branch Water; ZMCW: Zhe-min Coastal Water; M1: Quanzhou Bay Buoy; M2: Dagang Bay Buoy; R: river.

2.2. Mooring and field observations

Oceanographic and atmospheric properties were monitored at two mooring sites in Quanzhou coastal waters (Fig. 1). Observational data from Quanzhou Buoy (M1) included winds, chlorophyll *a*, and water velocity at the surface; at Dagang Bay Buoy (M2), water temperature and salinity at the surface were obtained. These data were obtained from the Fujian Province Marine Observation Demonstration Network (http://www.fjhyyb.cn/Ocean863Web_MAIN/default.aspx#hygc). Daily averages throughout the two study periods (May 20 to June 18, 2017 and 2018) were calculated based on hourly observations.

2.3. Remote satellite sensing measurements

Visible Infrared Imaging Radiometer Suite (VIIRS) ocean color and derived sea surface temperature level-2 data (L2) were downloaded from the NASA Goddard Flight Center (GSFC; http://oceancolor.gsfc.nasa.gov). The highest-quality L2 data were mapped to a cylindrical-equidistant projection at a ~1 km resolution using resampling.

During the pre-bloom and bloom events, we identified six dates with relatively high-quality images showing Fujian coastal waters (Fig. 5): May 30, June 10, and June 11 in 2017, and May 29, June 7, and June 9 in 2018.

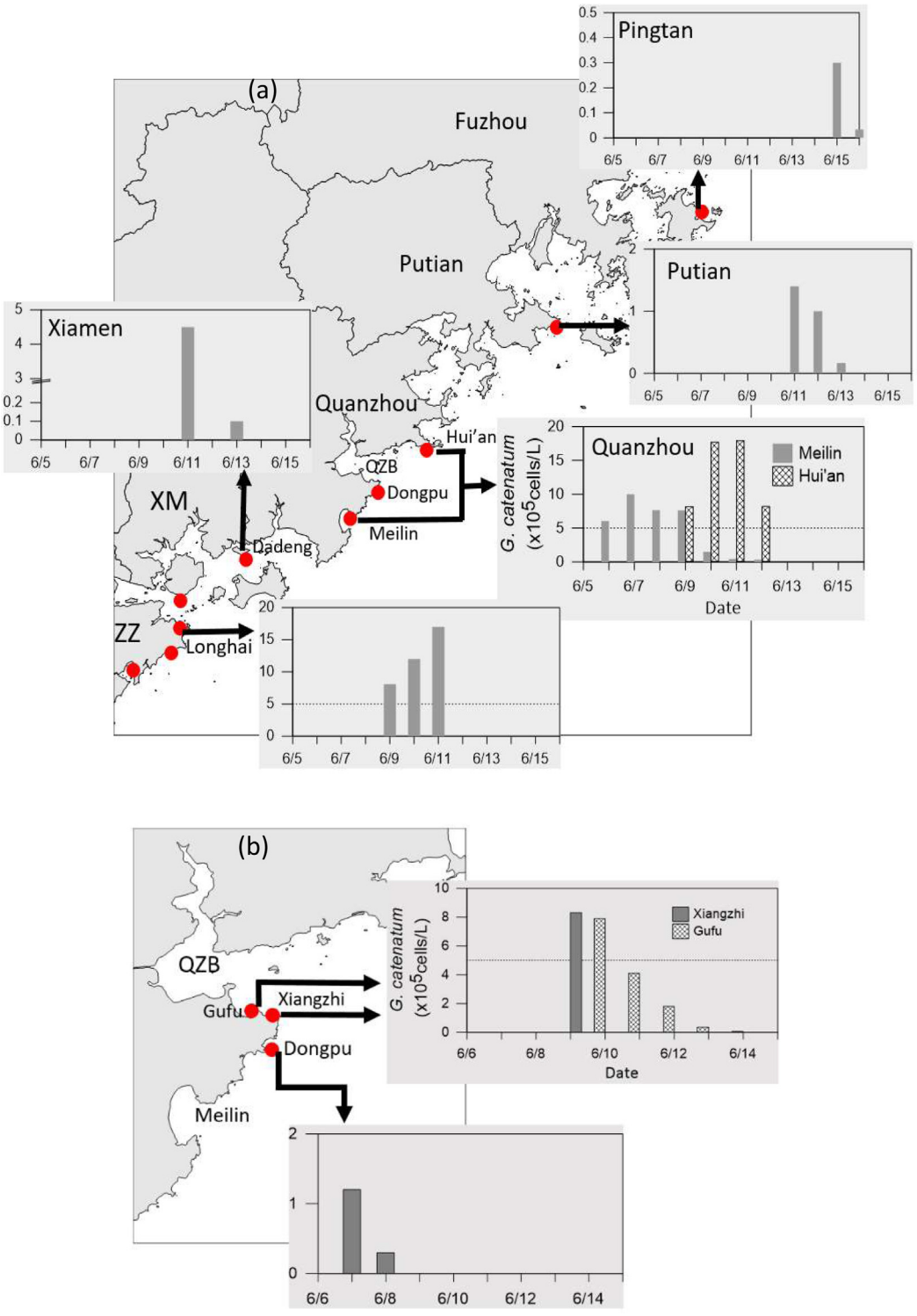

Fig. 2. Locations of *G. catenatum* blooms in June 2017 (a) and 2018 (b). The bar plots represent the temporal variations in the maximum concentrations of *G. catenatum* cells at selected monitoring stations. The dotted lines in the bar plots represent 5.0×10^5 cells/L. QZB: Quanzhou Bay; XM: Xiamen; ZZ: Zhangzhou.

Due to cloud cover, few VIIRS SST images of the TWS are available between May and June. Therefore, high-quality, three-day averaged data were used to improve SST coverage (Fig. 7).

2.4. Ekman transport

The Ekman transport variables Q_x and Q_y were calculated according to Cropper et al. (2014) as follows:

$$Q_x = \frac{\tau_y}{\rho_w f} = \frac{\rho_a C_d (W_x^2 + W_y^2)^{1/2} W_y}{\rho_w f}, \tag{2.1}$$

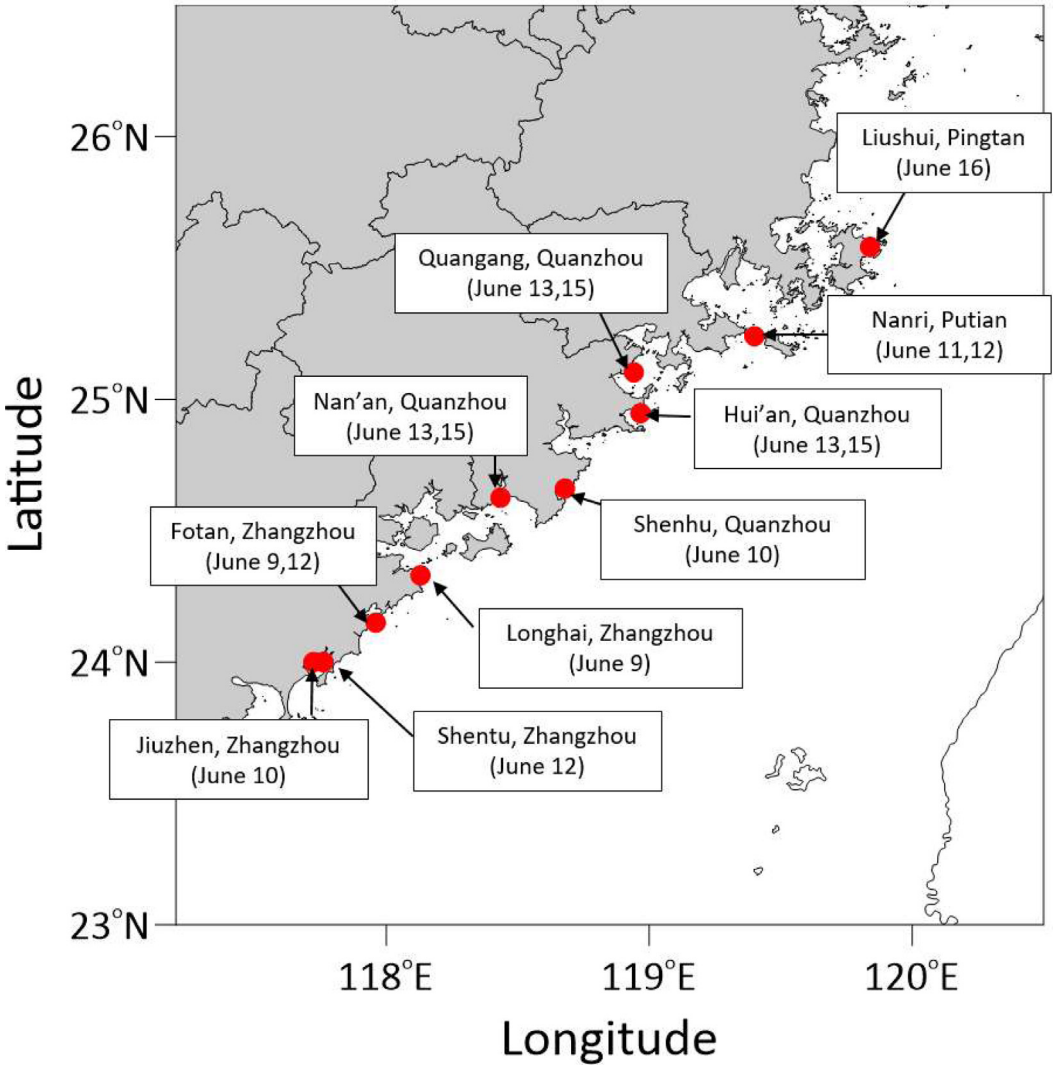

Fig. 3. Locations and dates at which the levels of paralytic shellfish poisoning toxin exceeded the regulatory limit.

and

$$Q_y = \frac{-\tau_x}{\rho_w f} = \frac{-\rho_a C_d (W_x^2 + W_y^2)^{1/2} W_x}{\rho_w f}, \tag{2.2}$$

where τ_x, τ_y are the zonal and meridional components of wind stress, ρ_a is the air density (1.22 kg m^{-3}), ρ_w is the seawater density (1025 kg m^{-3}), C_d is the dimensionless drag coefficient (1.3×10^{-3}), f is the local Coriolis parameter, and $W(W_x, W_y)$ is the wind speed near the surface.

To quantitatively describe the coastal upwelling conditions of the western TWS, the upwelling index (UI), which is defined as the Ekman transport (Q) component in the direction perpendicular to the shoreline, was calculated as follows:

$$\mathrm{UI} = Q_x \sin(\varphi) - Q_y \cos(\varphi), \tag{2.3}$$

where φ is the mean angle between the shoreline and the equator. UI also refers to the cross-shore Ekman transport. Positive values of UI indicate upwelling-favorable conditions, while negative values of UI indicate downwelling-favorable conditions (Cropper et al., 2014).

3. Results

3.1. Spatial–temporal variations in the G. catenatum blooms

The spatial–temporal variations in maximum *G. catenatum* cell concentrations along the Fujianese coast in early June 2017 and 2018 are shown in Fig. 2. In June 2017, the Zhangzhou and Quanzhou coastal areas were most severely affected by the *G. catenatum* blooms. On most sampling dates, the cell concentrations at these two locations exceeded the HAB threshold (5×10^5 cells L^{-1}), which were previously shown by Guo et al. (2005) to correspond to the onset of visibly discolored water. In addition to Zhangzhou and Quanzhou, *G. catenatum* were also observed in Xiamen Bay and in the Putian and Pingtan coastal areas. However, the cell concentrations at these locations were below the HAB threshold (Fig. 2a). Fig. 3 shows the location of the observation station where the PSP levels exceeded the regulatory limit. These results were collected from the daily HAB disaster information reports released by the OFBFJ. It can be inferred from Figs. 2 and 3 that up to 300 km of coastline, from Zhangzhou to Pingtan, were affected by *G. catenatum* in June 2017. The bloom subsided after June 12, possibly due to the strong winds and heavy rainfall associated with the typhoon "Merbok".

Conversely, blooms of *G. catenatum* in June 2018 were only observed in Quanzhou coastal waters. The impacted area, near

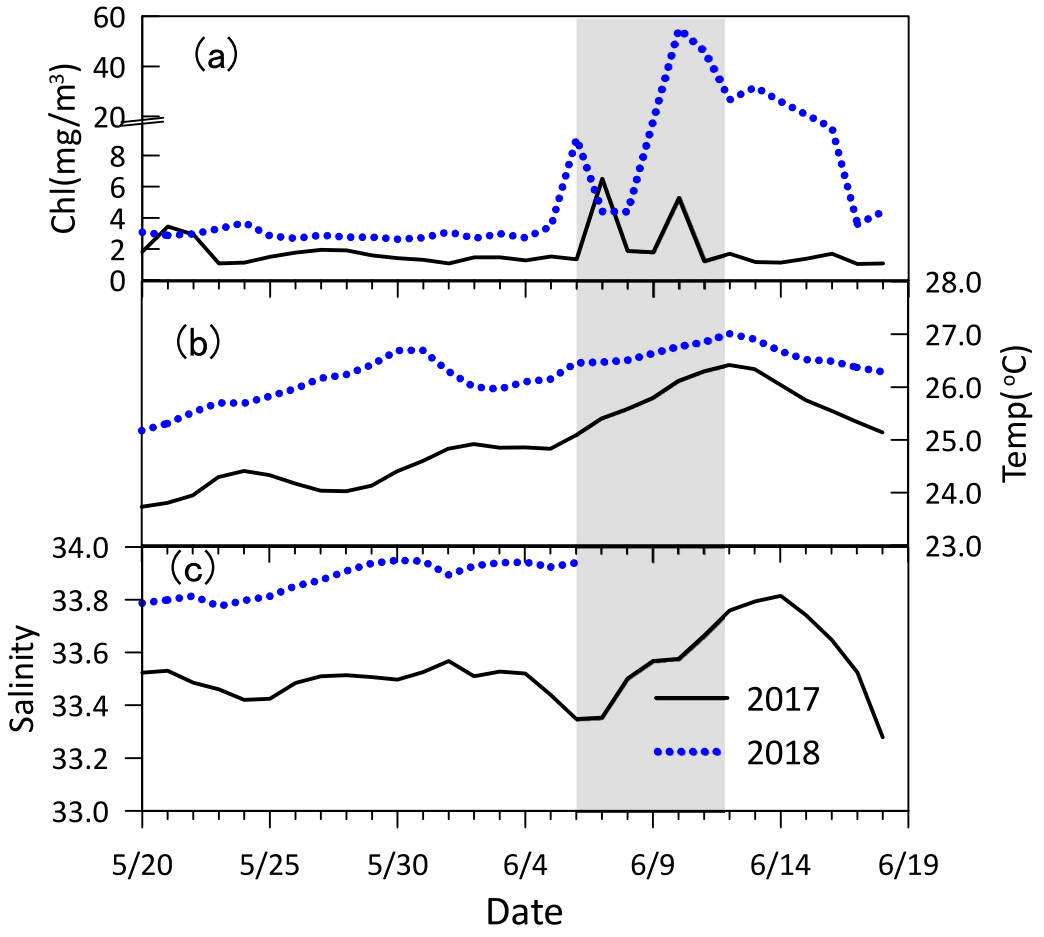

Fig. 4. Time series of chlorophyll a (a), temperature (b), and salinity (c), as observed at the mooring sites M1 and M2 from May 20 to June 18 in 2017 and 2018. The gray shading indicates the bloom period.

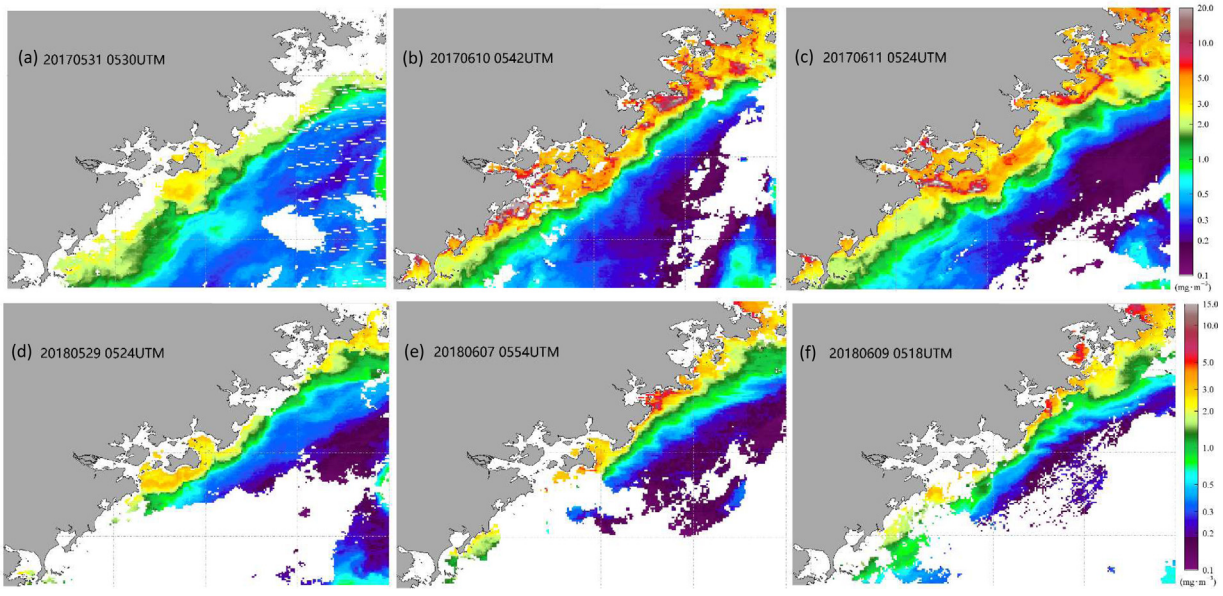

Fig. 5. Visible Infrared Imaging Radiometer Suite (VIIRS)-derived chlorophyll a images from 2017 ((a)–(c), top panel) and 2018 ((d)–(f), bottom panel).

the mouth of Quanzhou Bay (Fig. 2b), was much smaller than the impacted area in 2017. Unlike the 2017 HAB event, *G. catenatum* was not the dominant HAB species in 2018, and accounted for only about 1/10 of the total phytoplankton community (Haifeng Gu, in preparation). At the beginning of the bloom event (June 8), the average *G. catenatum* concentration was $<1.0 \times 10^5$ cells/L. The average concentration increased to 8.3×10^5 cells/L on June 9. The *G. catenatum* concentrations between June 9 and June 10 exceeded the HAB threshold (Fig. 2b). Fortunately, the area affected by the 2018 event was limited to a small embayment

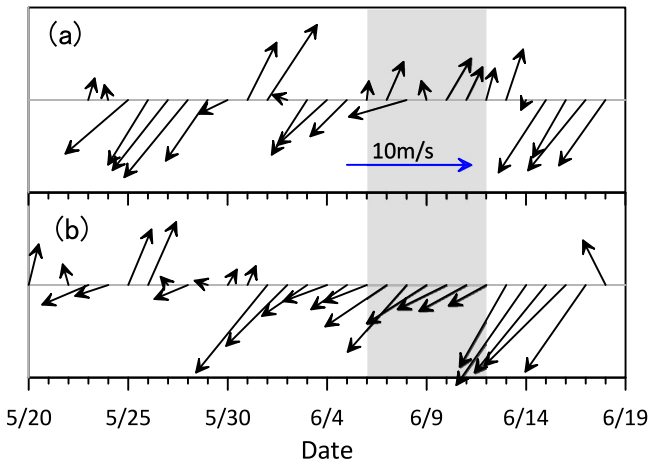

Fig. 6. Time series data for wind vectors, as observed by buoy M1 in 2017 (a) and 2018 (b). The gray shading indicates the bloom period.

in Quanzhou Bay (Fig. 2b), which is distant from areas of marine aquaculture (Huorong Chen, Oceanic and Fishery Bureau of Fujian Province; personal communication). Thus, this event did not result in the severe levels of shellfish contamination observed in 2017. The weakening of the HAB in the middle of June 2018 may have been due to the strong and persistent northeast winds after June 12 (Fig. 6b).

3.2. Changes in chlorophyll a concentration

The mooring-observed Chl *a* concentrations in June 2017 and 2018 were divided into three groups: before the bloom (May 31–June 5), during the bloom (June 6–12), and after the bloom (June 13–18; Fig. 4a; Table 1). Chl *a* increased during the blooms (June 6–12) in both 2017 and 2018 (Fig. 4a). During this period in 2017, Chl *a* levels doubled; during the same period in 2018, Chl increased nearly 10-fold, from 2.89 mg/m^3 to 22.67 mg/m^3. These temporal variations were basically consistent with changes in the concentration of phytoplankton cells (Fig. 2). The average Chl *a* level during the bloom period was much greater in 2018 than in 2017, suggesting that the total phytoplankton concentration was also greater in 2018. In 2018, Chl *a* concentration remained high (i.e., 15.32 mg/m^3) after the HAB. The precise mechanisms underlying this phenomenon remain unclear, and further observations in the field are required.

Although the VIIRS-derived Chl *a* images from 2017 and 2018 were constrained by cloud cover (Fig. 5), it is still evident that Chl *a* concentrations nearshore during bloom periods (Fig. 5b and c, e and f) were much higher than nearshore levels before the bloom (Fig. 5a and d). Several patches with high Chl *a* levels were scattered between the Zhang Zhou and Putian coasts in June 2017 (Fig. 5b and c). Conversely, in June 2018, patches with high Chl *a* levels were only observed near Quanzhou Bay (Fig. 5e and f).

VIIRS Chl *a* imagery alone cannot be used to discriminate algal classes. Moreover, due to variable cloud cover and the contamination of coastal waters with colored, dissolved organic matter, there are unavoidable biases in the satellite-derived Chl *a* products (Zhang et al., 2006). However, the location of the patch with high Chl *a* levels, as revealed by remote sensing, was similar to the location of the *G. catenatum* bloom based on field measurements (Figs. 2 and 5).

3.3. Sea surface temperature and salinity

Temporal variations in temperature and salinity were measured at the mooring buoys between May 20 and June 18 in

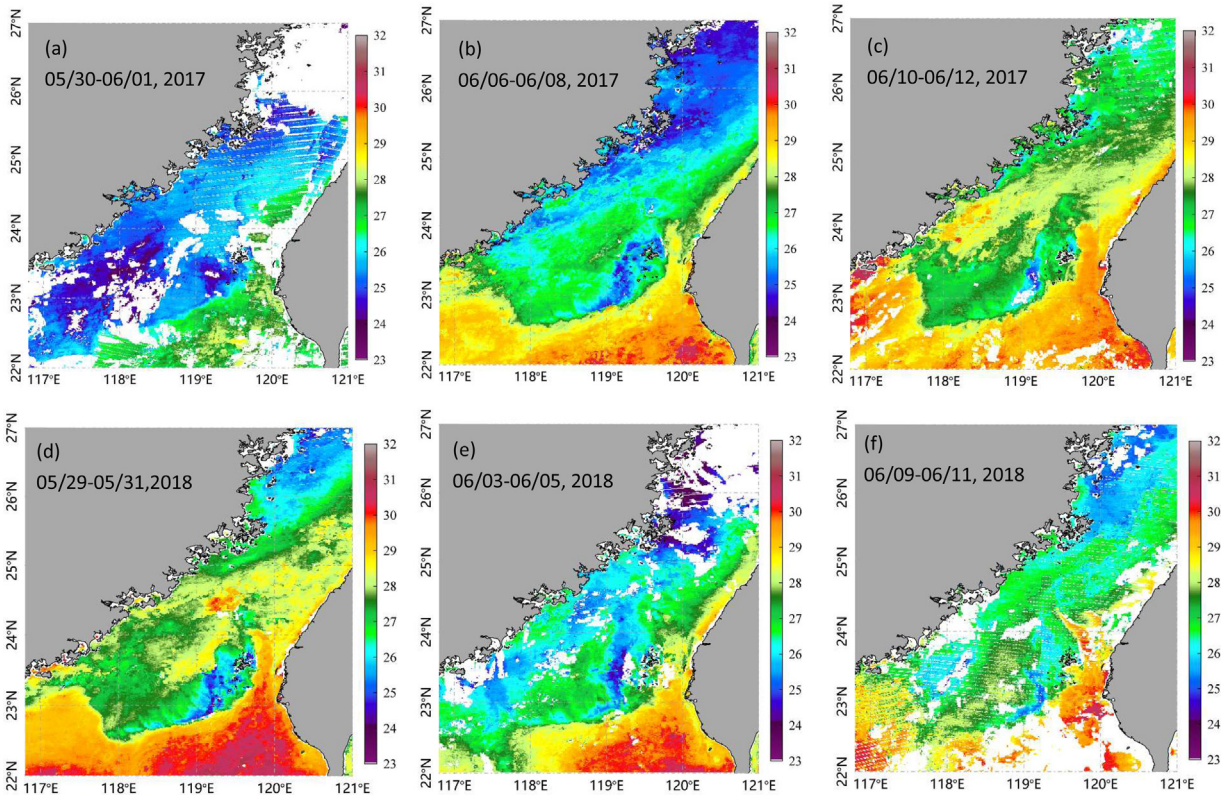

Fig. 7. Sea surface temperatures in 2017 (a–c, top panel) and 2018 (d–f, bottom panel), based on Visible Infrared Imaging Radiometer Suite (VIIRS) 3-day composite images.

Table 1
Mooring-observed surface temperatures, salinities, and chlorophyll *a* concentrations at three different stages during the bloom events.

	Before (5/30–6/5)		During(6/6–6/12)		After(6/13–6/18)	
	2017	2018	2017	2018	2017	2018
Temperature (°C)	24.76	26.27	25.82	26.67	25.69	26.54
Salinity	33.51	33.93	33.54	NA	33.63	NA
Chl (mg m^{-3})	1.36	2.89	2.82	22.67	1.25	15.32

2017 and 2018 (Fig. 4b and c; Table 1). In May and June of 2018, temperature and salinity were higher than in May and June of 2017 (Fig. 4 and Table 1). Temperature increased gradually from the end of May in both years, especially during the bloom events (June 6–12; Fig. 4; Table 1). Although the changes in salinity were not as significant as the changes in temperature, salinity also increased during the events. Both temperature and salinity decreased after the blooms. During the events (June 6–12) in 2017 and 2018, the average water temperature was 25.82 ° C and 26.67 ° C, respectively. In 2017, the average salinity was 33.54; the salinity during the 2018 bloom was not available.

The wind fields in May–June 2018 differed substantially from those in May–June 2017 (Fig. 6). In 2017, northeast winds dominated during the pre-bloom period, while southwest winds dominated during the bloom (Fig. 6a). However, in 2018, southwest winds dominated during pre-bloom period, while northeast winds dominated during the bloom period (Fig. 6b). In both years, the northeast wind dominated after the bloom.

The 3-day VIIRS SST images before and during the 2017 and 2018 bloom events revealed that hydrographic features differed noticeably between the years. During the 2017 pre-bloom period, the northwestern and central waters of the TWS were cool because the TWS was affected by the cold, fresh ZMCW under the control of northeast wind (Fig. 7a). During and after the HABs, the wind direction changed, increasing the strength of the influence of the Strait Warm Water from the south and increasing the temperature of the TWS (Figs. 7b, c). However, during the 2018 pre-bloom period, the area was affected by the warm, salty, oligotrophic Strait Warm Water (Fig. 7d). The SST decreased when the ZMCW intrusion became stronger, due to the influence of the northeast wind during the early bloom period (Fig. 7e). In the late bloom period, the northeast wind weakened, and the temperature rose slowly (Fig. 7e).

4. Discussion

The *G. catenatum* bloom in June 2017 was the first recorded in Fujianese waters (Chen, 2018). This weeklong algal bloom event, as well as its associated PSP toxins, impacted an extensive area: nearly 300 km, from Zhangpu to Pingtan (Figs. 2 and 3). During the blooms, *G. catenatum* cells tended to spread northward, as indicated by field and satellite observations (Figs. 2a, 3, 5b, c). In June 2018, the *G. catenatum* blooms impacted only a limited area near Quanzhou Bay, which was much smaller than the area affected by the 2017 event (Figs. 2b, 5e, f). The phytoplankton densities and Chl a levels increased significantly in two days (from June 8 to June 9, 2018; Fig. 2b & 4a).

Our investigations of the available observational data revealed one clear anomalous factor: wind forcing. As described in Section 3.3, the southwest wind prevailed during the 2018 pre-bloom period and then turned to the northeast during the bloom (Fig. 6b). However, in 2017, the northeast wind dominated during the pre-bloom period and shifted to a southwest wind during the bloom (Fig. 6a). The direction of surface circulation was generally consistent with wind direction (Fig. 8). This suggested that the surface circulation of the Taiwan Strait was mainly controlled by the wind, as has been demonstrated in previous studies (Hong et al., 2011; Jan et al., 2002).

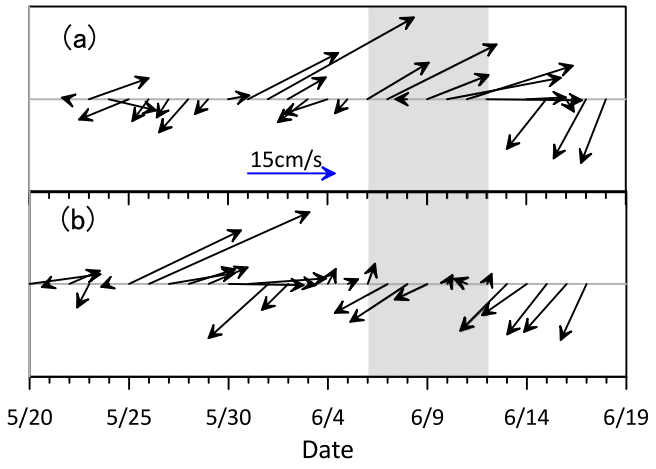

Fig. 8. Buoy observations showing time series data for the ocean currents in 2017 (a) and 2018 (b). The gray shading indicates the bloom period.

The short-term variations in the upwelling index (cross-shore Ekman transport) are shown in Fig. 9. Positive UI values represent upwelling-favorable conditions (offshore Ekman transport), while negative UI values represent downwelling-favorable conditions (shoreward Ekman transport). Clearly, the prevailing southwest wind in June 2017 was favorable for offshore transport and northward advection (Figs. 8a and 9a). Satellite-derived Chl *a* images (Fig. 5) revealed patches of high surface Chl *a* extending northeastward along the coast. These patches of high Chl *a* corresponded directly to the areas of the coastline where toxicity or population density levels were high (Figs. 2 and 3).

Based on our in situ and satellite observations (Figs. 2a, 3, and 5), we summarize the development of *G. catenatum* along the Fujianese coast in June 2017 as follows: the *G. catenatum* bloom first occurred at Zhangpu/Longhai on June 8–11, then moved to Xiamen Bay on June 11–13; at the same time, another bloom occurred at Meilin, Quanzhou, on June 6–9, spreading to Hui'an, Quanzhou, on June 9–11, to Nanri, Putian, on June 11–13, and finally to Pingtan on June 15–16.

Wind forcing is a key regulator of alongshore transport (Crespo and Figueiras, 2007; McGillicuddy et al., 2014). Moreover, upwelling-favorable winds tend to transport nearshore populations offshore, and downwelling-favorable winds tend to transport offshore populations shoreward (Franks and Anderson, 1992a,b; McGillicuddy et al., 2003). Inshore transport tends to result in the accumulation of cells in coastal waters (Tester et al., 1991). When we compared variations in UI and cell density and Chl *a* in 2018 (Figs. 2b and 9), it was clear that onshore transport weakened during the downwelling relaxation after June 8, 2018. Thus, *G. catenatum* cells might be brought into Quanzhou Bay due to the weakening of the northeast current. Simultaneously, onshore Ekman transport continued (Fig. 9), and current velocity decreased (Fig. 8). These hydrodynamic conditions not only favored the movement of populations from offshore areas to the inner bay but also inhibited the dispersal of the resulting algal aggregation due to the low current velocity.

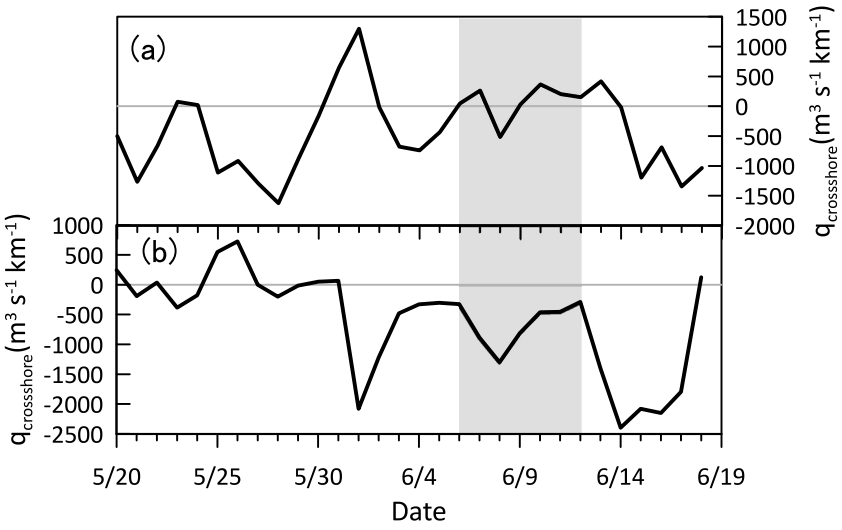

Fig. 9. Time series data for cross-shore Ekman transport (UI) from May 20 to June 18 in 2017 (a) and 2018 (b).

Nutrients are key to many HAB events (Kudela et al., 2010). During the bloom period in 2017, the UI remained mostly positive (Fig. 9), which indicated that the oceanic conditions in the TWS were favorable for upwelling. Upwelling is an important physical process that brings nutrient-rich deep waters to the upper surface of the TWS throughout the summer (Hong et al., 2011). Thus, upwelling might have provided the necessary nutrients for the development of the bloom in early June of 2017. Unfortunately, nutrient data were not available during the bloom period. Additional field observations are needed to assess the impact of nutrients on *G. catenatum* blooms. A previous study indicated that phytoplankton growth lagged 1–2 days behind summer upwelling activity in the Taiwan Strait (Shang et al., 2004). In early June 2017, the southwest wind lasted 1–2 days (Fig. 6a). Subsequently, *G. catenatum* cell concentrations peaked on June 7 and June 10–11 (Fig. 2). Thus, upwelling-favorable winds may play an important role in the enhancement of *G. catenatum* blooms. Consistent with this, several previous studies have also demonstrated that the dynamics of *G. catenatum* blooms are tightly coupled to upwelling (Bravo et al., 2010; Fraga et al., 1988; Moita et al., 2003; Trainer et al., 2010).

Our results also indicated that, in 2018, *G. catenatum* phytoplankton density increased from $<1.0 \times 10^5$ cells/L before June 9 to $>8.0 \times 10^5$ cells/L afterwards (Fig. 2b). Similarly, Chl *a* concentration increased from 2.89 mg/m^3 during the pre-bloom period to 22.67 mg/m^3 during the bloom (Table 1). Such substantial increases in phytoplankton densities and Chl *a* concentrations should require correspondingly large increases in nutrient supply. However, in 2018, the western TWS was influenced by the oligotrophic Strait Warm Water before the HAB event at the end of May (Fig. 7). Later in June, the ZMCW became stronger after the wind direction changed. However, nutrient concentrations in the coastal sea did not seem to increase significantly in this short time and thus seemed unlikely to provide sufficient support for the observed dramatic increases in Chl a levels and phytoplankton densities. Yin et al. (2008) also demonstrated that the nutrient concentrations in the surrounding waters were not high enough to support observed HAB cell densities and Chl *a* concentrations at that time. The authors hypothesized that this discrepancy might be explained by physical aggregation of algal cells due to wind and vertical dinoflagellate migration (Yin et al., 2008). This hypothesis was later supported by a physical–biological coupling model (Lai and Yin, 2014). Although *G. catenatum* has strong vertical migration behavior (Doblin et al., 2006), no measurements allowing us to evaluate these behaviors were made in the present study. Therefore, we hypothesize that physical aggregation, resulting from a combination of downwelling winds and *G. catenatum* vertical migration behaviors, were responsible for the sharp increase in phytoplankton density and Chl *a* in 2018.

Furthermore, the *G. catenatum* is a "mixing-drift" phytoplankton type (Smayda, 2000, 2002); such phytoplankton are adapted to the dynamic and rapidly-changing conditions that are forced by variability in coastal upwelling, including the high velocity zones of fronts, entrainment within coastal currents, and vertical mixing within upwelling relaxation (Ryan et al., 2009). *G. catenatum* probably dominated the HAB events of 2017 and 2018 because it can successfully adapt to energetic and variable upwelling/downwelling conditions. A more thorough evaluation of the mechanisms underlying *G. catenatum* bloom population dynamics will require further studies in the context of a three-dimensional hydrodynamic model.

In early summer, upwelling-favorable and downwelling-favorable winds alternate over short time scales because the southwest monsoon has just been established. The fluctuations in wind direction at event scales may be important in the transport and development of HAB populations in coastal upwelling systems (Fraga et al., 1988; Ryan et al., 2009; Pitcher et al., 2010). The alongshore currents driven by upwelling-favorable (southwest) winds moved the HAB northward, while downwelling-favorable (northeast) winds intensified the bloom via onshore transport and physical aggregation in the inner bay. During the transitional period of wind direction reversals, the nearshore flows slowed (Fig. 6). Furthermore, coastline features, such as capes and embayments, may interact with wind forcing to alter the general circulation patterns of upwelling systems at various spatial scales, resulting in the areas of convergence or retention (Figueiras et al., 2006). These processes may favor the development of high biomass blooms.

Here, we propose a conceptual model of HAB formation and persistence along the Fujianese coast (Fig. 10). When the southwest wind prevails, the bloom-forming algae are transported offshore with alongshore currents. The populations may affect the coastline due to coastal morphology. When the northeast wind is dominant, onshore transport leads to onshore population accumulation, possibly in coastal bays or fjords. The slow flow rate and long residence time of the semi-enclosed coastal bays or fjords may then provide suitable conditions under which algal

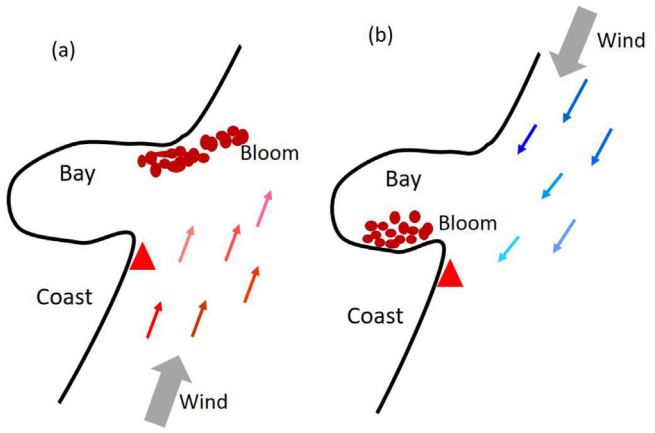

Fig. 10. Conceptual model showing how (a) southwest (b) northeast winds drove the *G. catenatum* bloom along the Fujian coast. The red triangle indicates where the bloom first occurred. The gray arrows indicate wind direction. The blue arrows represent the cold Zhe-Min coastal current. The red arrows represent the Strait Warm Water. The red dots represent the bloom distribution due to the wind.. (For interpretation of the references to color in this figure legend, the reader is referred to the web version of this article.)

cells are more likely to accumulate and less likely to disperse (Cembella et al., 2005; Lai and Yin, 2014). These environmental conditions might result in a high-intensity HAB.

The coastline of Fujian Province is tortuous and includes many harbors (Fig. 1); many aquaculture areas are distributed inside or outside these harbors. About one-third of the regional HAB events occur in June (Li, 2012). Thus, whether cells are transported onshore or offshore, the safety of aquaculture areas could be threatened. The extent and intensity of the HAB depended on the wind direction.

Although the precise mechanisms resulting in *G. catenatum* blooms remain unknown, our field observations demonstrated that alongshore transport driven by upwelling winds, as well as physical aggregation driven by downwelling winds and swimming behaviors, play important roles in HAB distributions and dynamics. Wind-associated physical transport and aggregation processes should be carefully considered during coastal management assessments, both for the development of HAB adaptation strategies and when projecting HAB risks for coastal areas.

Cysts, the "seed stocks" of red tides, also play an important role in the occurrence, persistence, and termination of red tide blooms (Anderson et al., 2012). A previous study observed *G. catenatum* cysts at only 1 of the 14 stations in South China Sea (Dapeng Bay; (Qi et al., 1996). However, recent studies have detected *G. catenatum* cysts (albeit in low concentrations) in the Bohai Sea, Yellow Sea, East China Sea, and South China Sea (Gu et al., 2011, 2013; Wang et al., 2004). With respect to Fujianese coastal waters, *G. catenatum* cysts were found in Xiamen Bay in 2000 (Lin et al., 2002). Unfortunately, no observational data regarding *G. catenatum* cyst distributions prior to the HAB outbreak in June 2017 are available. The HAB events in June 2017 and 2018 were so dense and extensive that cyst abundance and distribution along the Fujianese coast have already increased (Haifeng Gu, personal observations), and these cysts might well initiate future toxic HABs. Clearly, routine monitoring of toxic *G. catenatum* populations and cysts along the Fujianese coast should be continued and intensified.

5. Conclusion

Two intense HABs of the toxic dinoflagellate *G. catenatum* occurred along the coast of Fujian, China, in early June of 2017 and 2018. The 2017 bloom event was the first record of a *G. catenatum* bloom along the Fujianese coast. This event led to several PSP cases (44 individuals hospitalized), and resulted in the closure of many aquaculture farms. In 2017, the area in which *G. catenatum* and PSP exceeded the regulatory limits extended over ~300 km of coastline. In contrast, the area impacted in 2018 was much smaller and was limited to Quanzhou Bay. However, chlorophyll *a* concentrations and phytoplankton densities increased sharply over short periods during this event. Field measurements and remote satellite sensing data highlighted the importance of wind-driven alongshore transport and physical aggregation to the distributions and dynamics of these bloom events. Specifically, alongshore currents driven by upwelling-favorable (southwest) winds moved *G. catenatum* populations northward, and downwelling-favorable (northeast) winds intensified the bloom via onshore transport and physical aggregation in the inner bay in 2018. These wind-associated factors help to explain the differences in HAB impact area and intensity between 2017 and 2018. However, the complex mechanisms underlying *G. catenatum* bloom population dynamics require further studies in the context of a three-dimensional hydrodynamic model. The correlations between wind-driven hydrodynamic conditions and the HAB events of 2017 and 2018 identified herein improve our ability to predict *G. catenatum* blooms along the Fujianese coast and may thereby reduce the negative impacts of future HAB events.

CRediT authorship contribution statement

Caiyun Zhang: Conceptualization, Methodology, Writing - original draft. **Po-teen Lim:** Writing - review & editing. **Xueding Li:** Data curation. **Haifeng Gu:** Writing - review & editing. **Xing Li:** Data curation. **Donald M. Anderson:** Writing - review & editing.

Declaration of competing interest

The authors declare that they have no known competing financial interests or personal relationships that could have appeared to influence the work reported in this paper.

Acknowledgments

This work was supported jointly by the National Key Research and Development Program of China (# 2016YFE0202100 and 2016YFC1401906), Key Program of NSF-China (#U1805241), China Scholarship Council (#201806315023), MEL-XMU Internal Program (#MELRI1905), and MEL-XMU Visiting Fellowship (#MELRS1929). MODIS and VIIRS data were provided by the NASA Ocean Biology Processing Group (OBPG) through an online data portal (http://oceancolor.gsfc.nasa.gov). Support to DMA was provided by the National Science Foundation [OCE-1840381] and the National Institute of Environmental Health Sciences [1-P01-ES028938-01] through the Woods Hole Center for Oceans and Human Health. Support was also provided by ECOHAB project NOAA NOS #NA15NOS4780181. The authors also thank the Editor and two anonymous Reviewers for their insightful comments and valuable suggestions.

References

Anderson, D.M., 1989. Toxic algal blooms and red tides: a global perspective.. In: T., O., D.M., A., T., N. (Eds.), RedTides: Biology, Environmental Science and Toxicology. Elsevier, New York, pp. 1–16.

Anderson, D.M., 1995. Toxic red tides and harmful algal blooms- a pratical challenge in coastal oceanography. Rev. Geophys. 33, 1189–1200.

Anderson, D.M., Cembella, A.D., Hallegraeff, G.M., 2012. In: Carlson, C.A., Giovannoni, S.J. (Eds.), Progress in UnderstandIng Harmful Algal Blooms: Paradigm Shifts and New Technologies for Research, Monitoring, and Management. In: Annual Review of Marine Science, vol. 4, pp. 143–176.

Anderson, D.M., Jacobson, D.M., Bravo, I., Wrenn, J.H., 1988. The unique, microreticulate cyst of the naked dinoflagellate *Gymnodinium Catenatum*. J. Phycol. 24, 255–262.

Band-Schmidt, C.J., Morquecho, L., Lechuga-Deveze, C.H., Anderson, D.M., 2004. Effects of growth medium, temperature, salinity and seawater source on the growth of *Gymnodinium catenatum* (Dinophyceae) from Bahia Concepcion, Gulf of California, Mexico. J. Plankton Res. 26, 1459–1470.

Bolch, C.J.S., de Salas, M.F., 2007. A review of the molecular evidence for ballast water introduction of the toxic dinoflagellates *Gymnodinium catenatum* and the *Alexandrium tamarensis complex* to Australasia. Harmful Algae 6, 465–485.

Bravo, I., Fraga, S., Figueroa, R.I., Pazos, Y., Massanet, A., Ramilo, I., 2010. Bloom dynamics and life cycle strategies of two toxic dinoflagellates in a coastal upwelling system (NW Iberian Peninsula). Deep-Sea Res. Part II-Top. Stud. Oceanogr. 57, 222–234.

Cembella, A.D., Ibarra, D.A., Diogene, J., Dahl, E., 2005. Harmful algal blooms and their assessment in Fjords and coastal embayments. Oceanography 18, 158–171.

Chen, H.R., 2018. Emergency treatment and refletion of red tide event of *Gymnodinium Catenatum* in Fujian sea area in 2017. J. Fish. Res. 40, 308–314.

Crespo, B.G., Figueiras, F.G., 2007. Spring poleward current and its influence on microplankton assemblages and harmful dinoflagellates on the western Iberian coast. Harmful Algae 6, 686–699.

Crespo, B.G., Figueiras, F.G., Groom, S., 2007. Role of across-shelf currents in the dynamics of harmful dinoflagellate blooms in the northwestern iberian upwelling. Limnol. Oceanogr. 52, 2668–2678.

Cropper, T.E., Hanna, E., Bigg, G.R., 2014. Spatial and temporal seasonal trends in coastal upwelling off Northwest Africa, 1981-2012. Deep-Sea Res. Part I-Oceanogr. Res. Pap 86, 94–111.

Doblin, M.A., Thompson, P.A., Revill, A.T., Butler, E.C.V., Blackburn, S.I., Hallegraeff, G.M., 2006. Vertical migration of the toxic dinoflagellate *Gymnodinium catenatum* under different concentrations of nutrients and humic substances in culture. Harmful Algae 5, 665–677.

Du, Q., Zhang, Y.Q., Gao, L., Qian, X.M., Xu, C.Y., 2002. Characteristics and prevention of red tide in Fujian coast in recent years. J. Fujian Fish. 3, 2–37.

Estrada, M., Sánchez, F.J., Fraga, S., 1984. Gymodinium catenatum Graham en las rías gallegas (NO de España). Inv. Pesq 48, 31–40.

Fermín, E.G., Figueiras, F.G., Arbones, B., Villarino, M.L., 1996. Short-time scale development of a *Gymnodinum catenatum* population in the Ria De Vigo(NW Spain). J. Phycol. 32, 212–221.

Figueiras, F.G., Pitcher, G.C., Estrada, M., 2006. Harmful algal bloom dynamics in relation to physical processes. In: Graneli, E., Turner, J.T. (Eds.), Ecology of Harmful Algae. In: Ecological Studies, vol. 189, Springer-Verlag, Berlin, pp. 127–138.

FPBS (Fujian Provincial Bureau of Statistics), 2018. Fujian Statistical Yearbook. China Statistics Press, Beijing (in Chinese).

Fraga, S., Anderson, D.M., Bravo, I., Reguera, B., Steidinger, K.A., Yentsch, C.M., 1988. Influence of upwelling relaxation on dinoflagellates and shellfish toxicity in Ria-De-Vgo, Spain. Estuar. Coast. Shelf Sci. 27, 349–361.

Franks, P.J.S., Anderson, D.M., 1992a. Alongshore transport of a toxic phytoplankton bloom in a buoyancy current: *Alexandrium tamarense* in the Gulf of Maine. Mar. Biol. 112, 153–164.

Franks, P.J.S., Anderson, D.M., 1992b. Toxic phytoplankton blooms in the southwestern Gulf of Maine: testing hypothesis of physical control using historical data. Mar. Biol. 112, 165–174.

Graham, H.W., 1943. Gymnodinium catenatum, a new dinoflagellate from the Gulf of California. Tran. Am. Microsc. Soc. 62, 259–261.

Gu, H., Liu, T., Lan, D., 2011. Progress of dinoflagellate cyst research in the China seas. Biodivers. Sci. 19, 779–786.

Gu, H., Liu, T., Vale, P., Luo, Z., 2013. Morphology, phylogeny and toxin profiles of *Gymnodinium inusitatum* sp. nov. Gymnodinium catenatum and *Gymnodinium microreticulatum* (Dinophyceae) from the Yellow Sea, China. Harmful Algae 28, 97–107.

Guo, H., Zhou, Q.L., Zhao, D.Z., Xu, K.C., Wang, J.G., Wu, S.S., Yan, Q.L., Huang, X.Q., Han, G.C., 2005. Technical Specification for Red Tide Monitoring. Standards Press of China, Beijing.

Hallegraeff, G.M., 1993. A review of harmful algal blooms and their apparent global increase. Phycologia 32, 79–99.

Hallegraeff, G.M., Blackburn, S.I., Doblin, M.A., Bolch, C.J.S., 2012. Global toxicology, ecophysiology and population relationships of the chainforming PST dinoflagellate *Gymnodinium catenatum*. Harmful Algae 14, 130–143.

Hong, H.S., Chai, F., Zhang, C.Y., Huang, B.Q., Jiang, Y.W., Hu, J.Y., 2011. An overview of physical and biogeochemical processes and ecosystem dynamics in the Taiwan Strait. Cont. Shelf Res. 31, S3–S12.

Hong, H.S., Zhang, C.Y., Shang, S.L., Huang, B.Q., Li, Y.H., Li, X.D., Zhang, S.M., 2009. Interannual variability of summer coastal upwelling in the Taiwan Strait. Cont. Shelf Res. 29, 479–484.

Hu, J., Kawamura, H., Li, C., Hong, H., Jiang, Y., 2010. Review on current and seawater volume transport through the Taiwan Strait. J. Oceanogr. 66, 591–610.

Jan, S., Wang, J., Chern, C.-S., Chao, S.-Y., 2002. Seasonal variation of the circulation in the Taiwan Strait. J. Mar. Syst. 35, 249–268.

Kudela, R.M., Seeyave, S., Cochlan, W.P., 2010. The role of nutrients in regulation and promotion of harmful algal blooms in upwelling systems. Prog. Oceanogr. 85, 122–135.

Lai, Z., Yin, K., 2014. Physical–biological coupling induced aggregation mechanism for the formation of high biomass red tides in low nutrient waters. Harmful Algae 31, 66–75.

Li, X.D., 2012. Analysis on characteristics of red tide in fujian coastal waters during the last 10years. Environ. Sci. 33, 2210–2216.

Lin, Y.S., Cao, W.Q., Sameer, T., Zhang, Q., Qi, Y.Z., 2002. Studies on dinoflagellate cysts and their distibution in Xiamen Western Harbour. Oceanol. Limnol. Sin. 33, 407–414.

Mackenzie, L., Beauchamp, T., 2001. Gymnodinium Catenatum in New Zealand: A New Problem for Public Health and the Shellfish Industry. Cawthron Report, Cawthron Research Institute, New Zealand, p. 10.

Matsuoka, K., Fukuyo, Y., 1994. Geographical distribution of the toxic dinoflagellate *Gymnodinium catenatum* Graham in Japanese coastal waters. Bot. Mar 37, 495–503.

McGillicuddy, D.J., Brosnahan, M.L., Couture, D.A., He, R., Keafer, B.A., Manning, J.P., Martin, J.L., Pilskaln, C.H., Townsend, D.W., Anderson, D.M., 2014. A red tide of *Alexandrium fundyense* in the Gulf of Maine. Deep-Sea Res. Part II-Top. Stud. Oceanogr. 103, 174–184.

McGillicuddy, D.J., Signell, R.P., Stock, C.A., Keafer, B.A., Keller, M.D., Hetland, .R.D., Anderson, D.M., 2003. A mechanism for offshore initiation of harmful algal blooms in the coastal Gulf of Maine. J. Plankton Res. 25, 1131–1138.

Moita, M.T., Oliveira, P.B., Mendes, J.C., Palma, A.S., 2003. Distribution of chlorophyll a and *Gymnodinium catenatum* associated with coastal upwelling plumes off central Portugal. Acta Oecologica 24, S125–S132.

Pitcher, G.C., Figueiras, F.G., Hickey, B.M., et al., 2010. The physical oceanography of upwelling systems and the development of harmful algal blooms. Progr. Oceanogr. 85 (1–2), 5–32.

Qi, Y.Z., Hong, Y., Zheng, L., Kulis, D.M., Anderson, D.M., 1996. Dinoflagellate cysts from recent marine sediments of the South and East China Seas. Asian Mar. Biol. 13, 87–103.

Ryan, J.P., Fischer, A.M., Kudela, R.M., Gower, J.F., King, S.A., Marin I.I.I., R., Chavez, F.P., 2009. Influences of upwelling and downwelling winds on red tide bloom dynamics in Monterey Bay, California. Cont. Shelf Res. 29 (5–6), 785–795.

Shang, S.L., Zhang, C.Y., Hong, H.S., Shang, S.P., Chai, F., 2004. Short-term variability of chlorophyll associated with upwelling events in the Taiwan Strait during the southwest monsoon of 1998. Deep Sea Res. Part II: Top. Stud. Oceanogr. 51 (10–11), 1113–1127.

Smayda, T.J., 2000. Ecological features of harmful algal blooms in coastal upwelling systems. S. Afr. J. Mar. Sci. 22, 219–253.

Smayda, T.J., 2002. Turbulence, watermass stratification and harmful algal blooms: an alternative view and frontal zones as pelagic seed banks. Harmful Algae 1 (1), 95–112.

Sordo, I., Barton, E.D., Cotos, J.M., Pazos, Y., 2001. An inshore poleward current in the NW of the iberian peninsula detected from satellite images, and its relation with *G. catenatum* and *D. acuminata* blooms in the Galician Rias. Estuar. Coast. Shelf Sci. 53, 787–799.

Tang, D., Kester, D.R., Ni, I.H., Qi, Y., Kawamura, H., 2003. In situ and satellite observations of a harmful algal bloom and water condition at the Pearl River estuary in late autumn 1998. Harmful Algae 2, 89–99.

Tester, P.A., Stumpf, R.P., Vukovich, F.M., Fowler, P.K., Turner, J.T., 1991. An expatriate red tide bloom - transport, distribution, and persistence. Limnol. Oceanogr. 36, 1053–1061.

Tilstone, G., Figueiras, F., Fraga, F., 1994. Upwelling-downwelling sequences in the generation of red tides in a coastal upwelling system. Mar. Ecol.-Prog. Ser. 112, 241–253.

Trainer, V.L., Pitcher, G.C., Reguera, B., Smayda, T.J., 2010. The distribution and impacts of harmful algal bloom species in eastern boundary upwelling systems. Prog. Oceanogr. 85, 33–52.

Wang, Z.H., Matsuoka, K., Qi, Y.Z., Chen, J.F., 2004. Dinoflagellate cysts in recent sediments from Chinese coastal waters. Mar. Ecol. 25, 289–311.

Yan, T., Zhou, M.J., Zou, J.Z., 2002. A national report on harmful algal blooms in China. In: Taylor, F.J.R.M., Trainer, V.L. (Eds.), Harmful Algal Blooms in the PICES Region of the North Pacific, Sidney. B.C. Canada, pp. 21–37.

Yin, K., Song, X.X., Liu, S., Kan, J., Qian, P.Y., 2008. Is inorganic nutrient enrichment a driving force for the formation of red tides? A case study of the dinoflagellate *Scrippsiella trochoidea* in an embayment. Harmful Algae 8, 54–59.

Yu, R., Luo, X., 2016. Status and research perspectives on toxic algae and phycotoxins in the coastal waters of China. Stud. Mar. Sinica 51, 155–166.
Zhang, C.Y., Hong, H.S., 2014. Interannual variability of remotely sensed chlorophyll a during an autumn monsoon transitional period in the Taiwan Strait. Acta Oceanol. Sin 33, 72–80.
Zhang, C.Y., Hong, H.S., Ru, C.M., Shang, S.L., 2011. Evolution of a coastal upwelling event during summer 2004 in the southern Taiwan Strait. Acta Oceanol. Sin 30, 1–6.
Zhang, C., Hu, C., Shang, S., Müller-Karger, F.E., Li, Y., Dai, M., Huang, B., Ning, X., Hong, H., 2006. Bridging between SeaWiFS and MODIS for continuity of chlorophyll-a concentration assessments off Southeastern China. Remote Sens. Environ. 102 (3–4), 250–263.
Zhou, M.j., Shen, Z.l., Yu, R.C., 2008. Responses of a coastal phytoplankton community to increased nutrient input from the Changjiang (Yangtze) River. Cont. Shelf Res. 28, 1483–1489.